Nigerian Journal of Engineering, Vol. 30, No. 1, April 2023, ISSN (print): 0794 – 4756, ISSN(online):2705-3954.

Nigerian Journal of Engineering,
Faculty of Engineering, Ahmadu Bello University, Zaria, Nigeria
journal homepage: www.njeabu.com.ng

Fog Attenuation Model Validation in the Tropical Climate using Machine Learning

D. Gambo*, A. M. S. Tekanyi, S. M. Sani, M. J. Musa, M. D. Al-Mustapha, I. Yau
Department of Electronics and Telecommunication Engineering Ahmadu Bello University, Zaria, Nigeria
* danasabegambo@gmail.com

Research Article

Abstract

A major technical challenge in FSOC systems is that their performance is limited by atmospheric impairments such as: absorption, scattering and turbulence caused by rain, cloud, snow, wind, dust, aerosol and fog. Many researches were carried out to improve the system through mathematical model and system development. The existing models (Kim and Kruse) performed poorly especially at low visibility portion ($v \leq 0.5\ km$), whereby, the coefficient of attenuation is wavelength independent as the value of particle size distribution coefficient is zero. Most of these researches were conducted in polar, continental, and temperate climates, while few are conducted on tropical climate. This research is aimed at addressing the challenges due to fog in a tropical climate through mathematical modeling and validation. The existing models were replicated and the test-bed also constructed for measurement as a means of validations. The new and improved models were developed, optimized, and simulated. The results obtained were compared with that of existing models, and it was observed that the developed model best fitted the measured result and achieved lower attenuation of 37.7% and 33.3% with respect to Kruse and Kim models respectably.

doi: 10.5455/nje.2023.30.01.09

Keywords
Fog, Attenuation, Particles Size Distribution Coefficients and Machine Learning.

Article History
Received: – December, 2022
Reviewed: – January, 2023
Accepted: – February, 2023
Published: – April, 2023

1. Introduction

The world is advancing, and communication devices have become more powerful and extensively adopted. The need for high data rate is increasing. This has led to spectrum scarcity in Radio Frequency (RF) systems. Consequently, it is necessary to explore other technical means to overcome the rising demand for higher data rates. Free Space Optical Communication (FSOC) offers one of such means. FSOC systems have the potential to offer much higher bandwidth than RF systems. In recent years, remarkable growth has been realized in communication industries (Kaushal and Kaddoum, 2016). The increasing usage and demand for high-speed internet, video conferencing and live streaming etc., has caused the demand for bandwidth to increase drastically. It has been revealed that, over 70% of the world population will become internet users by 2023. This is as a result of advancement achieved by electronics / t elecommunications sector. The number of subscribers expected to raise from around 5.1 billion (66 %) in 2018 to about 5.7 billion (71%) by the year 2023 (Cisco, 2020). as in Figure 1.

In the Nigerian context, the Nigerian Communications Commission (NCC) has placed the current broadband infiltration in the country at 33% in the year 2018 (NCC, 2020). Similarly, there are approximately 4.8 billion internet subscribers globally as at the second quarter of 2020, this represents a growing rate of 1239% in between the years 2000 to 2021 (NCC, 2020). This ever-growing demand for bandwidth and new emerging applications contribute to the scarcity of traditional Radio Frequency (RF) spectrum.

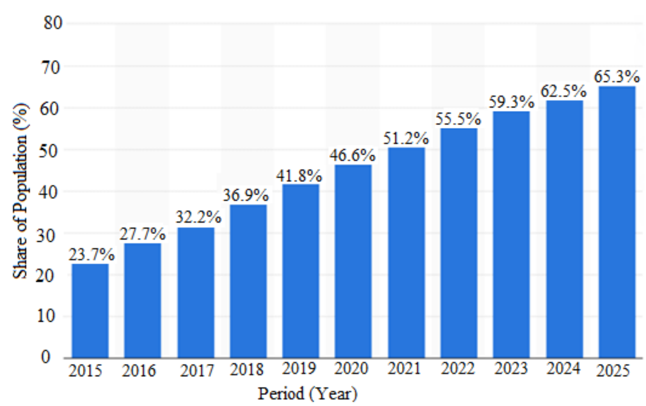

Figure 1: Global Internet Users Growth (Cisco, 2020).

Consequently, the need arose to explore alternatives that would help overcome the RF spectrum constraint. Among the few alternatives (massive MIMO, cognitive radio network etc,) to address the inherent challenge of the traditional RF is the Free-Space Optical Communication (FSOC). This is the main objective of this research. FSOC is the technology that ut ilizes the optical carriers to send information signal from one point to another through an unguided medium. Currently, FSOC has the potential to provide large bandwidth capable of providing high speed of multimedia communications through the atmosphere (Mingjian *et al.*, 2018). However, a major technical challenge in the FSOC systems is that, their performance is limited by atmospheric impairments such as: rain, cloud, snow, wind, dust, aerosol, and fog. This caused absorption, scattering, and turbulence in the medium which resulted in signal attenuation. This research aims at addressing the challenges due to fog, using mathematical modeling and simulation by means of machine learning.

FSOC require a line-of-sight linking between transmitter and receiver for the transmission of information from one point to another. The input signal from the source is modulated using the optical carrier, and the modulated signal is then transmitted through the atmospheric channel or free space, towards the receiver as illustrated in Figure 2 (Kaushal *et al.*, 2017).

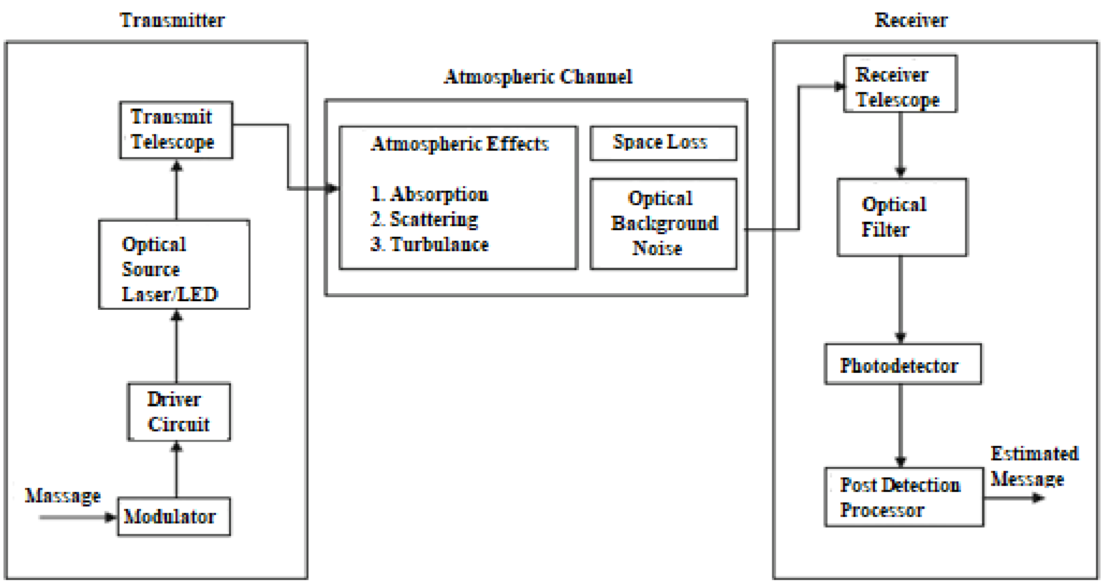

Figure 2: FSOC System Block Diagram (Kaushal *et al.*, 2017).

1.1 Related Works

Kashani *et al.*, illustrated that FSOC channels are influenced by atmospheric temperature that changes in both spatial and temporal domains. Esmail *et al*., developed a unified model for fog attenuation in FSOC links. Henniger and Wilfert, demonstrated that the key factors constituting signal degradation on the FSOC channel are fog, dust, and rain. Farouk *et al.*, analyzed the performance of FSOC channel under foggy weather condition using Kruse's and Kim's models. Jahid *et al.*, conducted a contemporary survey on FSOC systems to explore its potentials, technical challenges, current advances, and research direction. Gambo *et al.*, works on Mitigation of Beam Divergence Loss in FSOC Channel Using Field of View Technique.

It has been observed that, most of the reviewed works adopted Kim's and Kruse's models for their analysis. However, the models are wavelength independent at lower visibility range. Therefore, there is a need to develop new model or improve on the existing models used especially in the area of low visibility. This is the sole aim of this research.

1.2 Robustness and Benefits of FSOC

There are many features associated with FSOC system th at made it to be highly robust. These include: providing a virtually unlimited degree of frequency reuse in many conditions (Killinger, 2002). Secondly, FSOC adopts optical laser transmissions and travel along the line-of-sight path that cannot be interrupted easily, which add the degree of security to the system. Similarly, according to "fSONA" an FSOC firm at Canada, the cost per Mbps per month is approximately half that of RF-communication system (Rockwell & Mecherle, 2001). The primary advantages of FSOC over fiber are (Patnaik *at el.*, 2016).

i) Rapid deployment time and
ii) Significant cost savings
iii) Immune to EM Wave

1.3 FSOC and Feature Applications

The fifth-generation (5G) communication system is already deployed, while that of the upcoming sixth-generation (6G) expected to provide a higher quality of service (QoS) (Chowdhury *et al.*, 2019). The main requirement of 5G and 6G includes massive device connectivity, ultra-high security, low energy consumption, high system capacity, and low latency (Khalid *et al.*, 2019). Figure 3 illustrates how FSOC can provide solutions to 5G, 6G and IoT requirements (Qadir *et al.*, 2021).

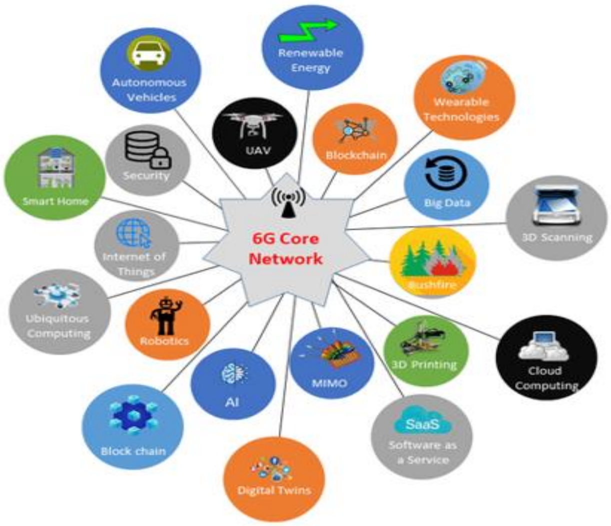

Figure 3: FSOC for 5G, 6G and IoT (Qadir *et al.*, 2021).

2. Technical Challenges

Despite the major advantages of FSOC, its widespread deployment is hindered by many challenges such as absorption, scattering and distortion. FSOC technology uses free space as its propagating medium whose properties are random functions of space and time. This makes FSOC a random phenomenon that is solidly dependents on atmosphere and geographical position as illustrated in Figure 4 (Kedar and Arnon, 2004).

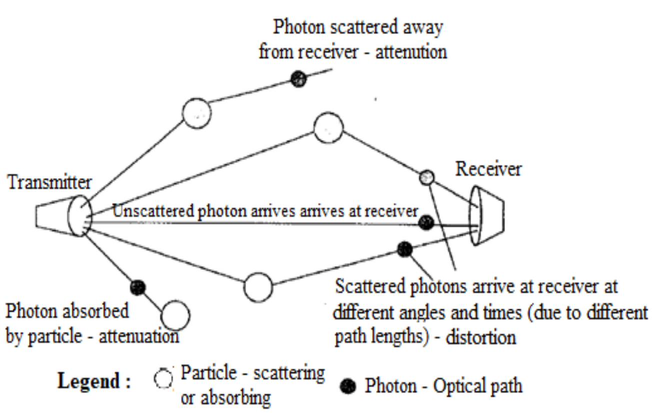

Figure 4: Spatial and Angular Spreading and Variation in Photon Path Length (Kedar & Arnon, 2004).

2.1 Absorption and Scattering

The attenuation experienced by the FSOC system are mainly due to absorption and scattering processes. At visible and Infrared (IR) wavelengths, the primary atmospheric absorbers are the molecules of water, carbon dioxide, and ozone (Ijaz *et al.*, 2013a). The loss experienced by the optical signal in the atmosphere can be computed in terms of optical depth τ which associates power at the receiver P_R with transmitted power P_T (Fang *et al.*, 2018) as:

$$\mathrm{P_R} = \mathrm{P_T}\exp(-\tau) \tag{1}$$

Where: τ is the ratio of the received to the transmitted power in the optical link which is also considered as atmospheric transmittance as in (2) (Ijaz *et al.*, 2013b):

$$T_a = P_R/P_T = \exp(-\tau) \tag{2}$$

where T_a is the transmittance and τ is the optical depth. Equation (3) and (4) relates the atmospheric attenuation coefficient γ and the propagation range R as in (Ijaz *et al.*, 2013b):

$$T_a = exp\left(\int_0^R (\rho)d\rho\right) \tag{3}$$

$$\tau = \int_0^R \gamma(\rho)d\rho \tag{4}$$

The loss in dB that the signal (light) experiences through propagation in the atmosphere is define by (5).

$$LOSS_{prop} = -10\log_{10} T_a \tag{5}$$

3. Methodology

The main aim of this research is to develop and validate the fog attenuation model in the tropical climate. This part of the research illustrates the step-by-step procedure on how the stated aim was achieved.

3.1 Fog Attenuation Modeling

Fog elements decrease the visibility close the ground. The meteorological meaning of fog is, when the visibility decreases to around 1 km (Ijaz *et al.*, 2012). The presence of condensed fog normally decreases the visibility as a result of scattering and absorption effects on the optical signal. Consequently, reduces the FSOC link distance to approximately 0.5 km (Ijaz *et al.*, 2012). Theoretically, the determination of fog attenuation can be possibly achieved by considering that, the fog particles are spherical. Mie theory can be applied to analyze the scattering over a cross section C_s of the particle, provided the radius r of the particle is known. Thus, the amount of the normalized scattering efficiency Qs can be estimated using (6) (Shaker and Ali, 2019) as:

$$Q_s = \frac{C_s}{\pi r^2} \tag{6}$$

Attenuation encouraged by the particles within the atmosphere is the sum total of the molecular absorption and scattering of light. But the wavelengths adopted in FSOC are carefully designated in the spectrum transmission windows
in order to minimize the molecular absorption. Therefore, the optical attenuation, β_λ, due to fog scattering is given by (Shaker and Ali, 2019) as:

$$\beta_\lambda = \int_0^\infty \pi r^2 Q_s\left(\frac{2\pi r}{\lambda}, n'\right) n(r)dr \tag{7}$$

Where, n' is the main real part of refractive index, and $n(r)$ is particle size distribution and λ is the wavelength.
The particles of fog in the atmosphere are random in nature which introduced complexity in fog attenuation estimation in terms of particles size and distribution. Consequently, empirical models using visibility data are the suitable and accurate means of estimation. In practice, the meteorological value of visual range (v) is the most important factor considered to analyzed the fog atten uation. Using the Koschmieder law, as in (8) Flecker *et al.*, 2015),

$$V = \frac{10 \log_{10} T_{th}}{\beta_\lambda} \tag{8}$$

Where T_{th} is visual threshold
Kruse developed an empirical relationship between v, β_λ and λ to minimize the complexity of determining the particle size and distribution. Fog parameter depends on wavelength of the propagation beam and visibility. Therefore, the attenuation due to fog can be predicted using (9).

$$\beta_\lambda = \frac{10 \log_{10} T_{th}}{V} \left(\frac{\lambda}{\lambda_o}\right)^{-q} \tag{9}$$

Where, λ is the wavelength, λ_o is the maximum spectrum of the solar band (550 nm). Where, q is the coefficient of particle size distribution given by Kruse (Killinger, 2002), as in (10):

$$q = \begin{cases} 1.6 & \text{for } v > 50 \text{ km} \\ 1.3 & \text{for } 6 < v < 50 \text{ km} \\ 0.585(\mathrm{V})^{1/3} & \text{for } 0 < v < 6 \text{ km} \end{cases} \tag{10}$$

However, the value of q in (10) determines using haze particles present in the atmosphere. Consequently, the Kruse model estimation considered to be inaccurate. Therefore, to amendthe presu med error, Kim modified Kruse model with some values of q as in (11) (Adel *et al.*, 2020), as:

$$q = \begin{cases} 1.6 & \text{for } v > 50 \text{ km} \\ 1.3 & \text{for } 6 < v < 50 \text{ km} \\ 0.16V + 0.34 & \text{for } 1 < v < 6 \text{ km} \\ v - 0.5 & \text{for } 0.5 < v < 1 \text{ km} \\ 0 & \text{for } v < 0.5 \text{ km} \end{cases} \tag{11}$$

Equation (9) in combination with (11) depicts that, the coefficient of attenuation β_λ is a wavelength independent at v $<$ 0.5 km where the value of q is 0. (Adel *et al.*, 2020), However, there is a need to optimize the related parameters at lower visibility region for the new value of q. This will help to further mitigate the attenuation effect caused by channel impairments.

3.2 Modelling and Simulation

Kim modified the Kruse model as in (11), which indicated that, the coefficient of attenuation β_λ is wavelength independent at v $<$ 0.5 km. However, as v reduces for any incident λ_{nm}, the value of q can be change by a factor X (v). Hence, there is need to modify the existing models by introducing a new buffer region for q, to investigate and improve on the existing model, especially in the region of low visibility (v $<$ 0.5), as in (12).

$$q = \begin{cases} 1.6 & \text{for V} > 50 \text{ km} \\ 1.3 & \text{for } 6 < V < 50 \text{ km} \\ 0.16V + 0.34 & \text{for } 1 < V < 6 \text{ km} \\ \mathrm{V} - 0.5 & \text{for } 0.5 < V < 1 \text{ km} \\ \mathrm{X(V)} & \text{for V} < 0.5 \text{ km} \end{cases} \tag{12}$$

To achieve the above proposed modification, there is need to further analyze the relationship between variables of Kruse model as in (9) such as; visibility, attenuation, particle size distribution and spectrum of the solar band, considering the governing assumptions as follows:

i) Attenuation is constant
ii) λ is constant

Therefore,

$$V = a\left(\frac{\lambda}{\lambda_o}\right)^{-q} \tag{13}$$

$$a = \frac{10 \log_{10} T_{th}}{\beta_\lambda} \tag{14}$$

Then, the proposed model equation can be written as in (15):

$$ln\, V = ln\, a + q ln\left(\frac{\lambda_o}{\lambda}\right) \tag{15}$$

Equation (15) is the linear representation of (9). Hence, the cost function or error function is given by

$$\mathrm{v}\left(\left(\frac{\lambda_o}{\lambda}\right), \mathrm{k}\right) = \frac{1}{\mathrm{n}}\sum_{\mathrm{i=1}}^{\mathrm{n}}\left[\mathrm{v}_i - \left(\left(\frac{\lambda_o}{\lambda}\right)_{\mathrm{i}} + \mathrm{k}\right)\right]^2 \tag{16}$$

In Gradient Decent Optimization (GDO) technique, k and $\left(\frac{\lambda_o}{\lambda}\right)$ of (16) represent the bias (B) and the weight (W) of the iterations of the optimization process respectively. Weight and bias as in (17) and (18) are to be deduced from the trained result to obtain the train model equation.
Therefore, the objective functions are (i) Loss < 0.5 and (ii) v < 0.5 km. This is to allow the predicted value of visibility (v_p) should not go beyond 0.5 km. Similarly, the lost function of 0.5 yield and accurate result.

3.3 Solving the Optimization Problem

This is the process of minimizing or maximizing a real function by methodically selecting the input values within the permissible set for computation to obtain better performance.

3.3.1 Gradient Descent Optimization (GDO)

Gradient Descent Optimization (GDO) technique is the optimization technique adopted for this research. The technique has the potentiality of automated reasoning to find the best fit. Secondly, it has a convergence control parameter (Learning rate). GDO supports both linear and non-linear functions automatically with the use of momentum in the complex function. It also uses an update rule to specified parameters over several iterations in an automated learning process. Therefore, it will be considered from the fundamental calculus concept for this research, with the following update rule given by (17) and (18), which will be used for iteration process (Garcia, 2018) as:

$$W = W - \mu h\dot{f}(L) \tag{17}$$

$$B = B - \mu h\dot{f}(L) \tag{18}$$

Where: W *is the weight*, B *is the bias*,

μ is the learning rate and *hf(L)* is first derivative of loss function

3.3.2 Python programming language

Python is an object-oriented programming language. It is perfectly designed for rapid prototyping of technical systems. It can be interfaced to many operating system calls and libraries. The high-level programming language couple with the running speed make the software more convenient and user friendly. This allows for the execution of gradient descent optimization (GDO) technique easily.

3.4 Experimental Measurement

The test-bed was successfully constructed as shown in Figure 5. The fog was artificially generated using the fog generator and then the signal sent from the developed optical transmitter and then received by the optical receiver at interval of distance. The procedure repeated several times. For each procedure the voltage and current sensors recorded the voltage and current and then saved it in the SD Card.

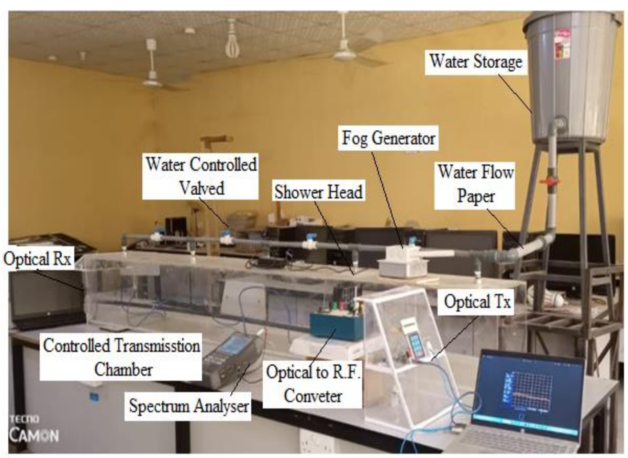

Figure 5: Constructed Test-bed illustration

3.4.1 Optical transmitter

The transmitter accepts the electrical signal at its input, manipulates the signal and then converts it into optical signal. Devices, such as LED or laser diode are been used to generates an optical signal suitable for transmission via an optical transmission medium. Figure 6 shown the developed optical transmitter circuit diagram.

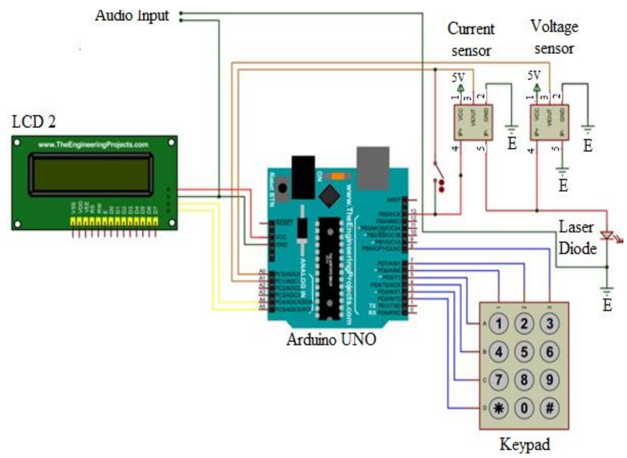

Figure 6: Optical Transmitter Circuit

3.4.2 Optical Receiver

FSOC systems utilize photodiode at the receiver to detect the sent signal from transmitter. However, photodiode has narrow receiver aperture which resulted in a serious optical signal lost due to beam divergence. To overcome the stated challenge a mini-solar panel with a wider aperture compared to that of the photodiode was introduced and served as a photo-detector. Figure 7 shown the optical receiver circuit diagram.

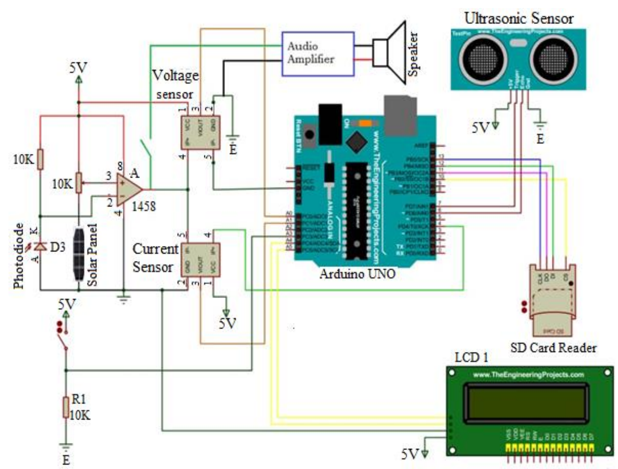

Figure 7: Optical Receiver Circuit

4. Results and Discussion

This section of the research presents the simulation as well as the optimization results of the existing (Kim and Kruse) models as well as that of the improved model. The aim is to investigate the performance of each model related to FSOC channel in the area of low visibility. The result obtained will be used to investigate how the developed model further mitigates the attenuation effects by comparing with that of the existing models.

4.1 Investigation of Kim and Kruse Models at Low Visibility ($v < 0.5$ km)

Equation (9) was used to simulate the relationship between low visibility and particle size distribution coefficient (q). This is for the purpose of investigating the performance of the existing models at low visibility.

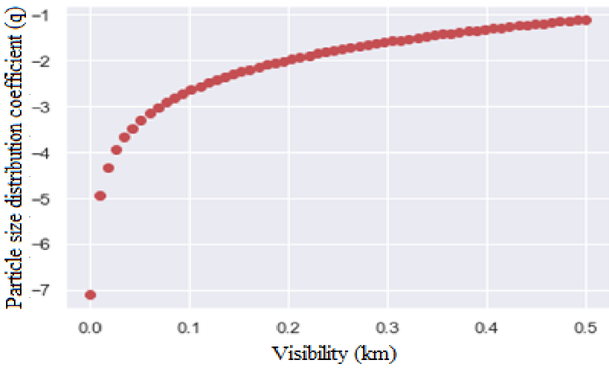

Figure 8: Particle size distribution coefficient against visibility

Figure 8 shows the relationship between particle size distribution coefficient (q) and low visibility of Km and Kruse models.

The result shows that the value of q is exponentially increases within the lower range of visibility ($0 < v \leq 0.5$ km). This conforms to the theoretical assumptions of both Kruse and Kim models whereby the highest value attained by q within the visibility range ($0 < v \leq 0.5$ km) is tends towards zero. This reveals the wavelength independency character of these models at lower visibility portion of the channel.

4.2 Optimization of the Developed Model at Low Visibility ($V \leq 0.5$ km)

The developed model equation (15) was optimized as shown in Equation (20). The purpose of this optimization is to maximize the particles size distribution coefficients (q) values within the area of low visibility for better performance. Figure 6 shows the relationship between low visibility and particle size distribution coefficient (q) of the developed model Equation.

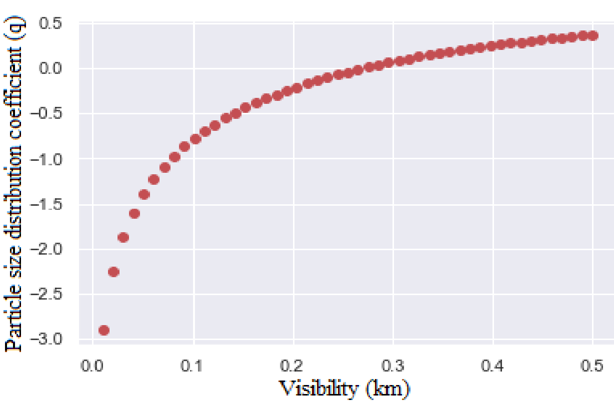

Figure 9: Particle Size Distribution Coefficient (q) against Low Visibility ($V \leq 0.5$ Km) of the Developed Model.

The optimization result in Figure 6 shows that the particles size distribution coefficient (q) has been maximized to some values beyond zero (0) at low visibility ($v < 0.5$ km). It has been observed that there is a significant improvement of approximately 0.4 maximum on the value of q in comparison with that of Kim and Kruse models as shown in Figure 9.

4.3 Determination of the Optimized empirical model at low visibility ($V \leq 0.5$ km)

The weight and bias as in Equations (17) and (18) were calculated to determine the optimized model that will best define the optimization curve of Figure 8 by empirical method. Equation. (19) is the optimization code in Phython that shows how weight (W), Bias (B) and particle size distribution coefficient (q) relates.

$$\text{Outputs (q)} = \text{Weight} * \text{np.log(inputs)} + \text{Bias} \quad (19)$$

The weight and bias were calculated. The obtained values were substituted in (19) to determine the optimized empirical model as in (20).

$$q = 0.773429 \ln(v) + 0.9074367 \quad (20)$$

Equation (20) is the optimized empirical model equation that perfectly defined the curved in Figure 8. Table 1 shows all the calculated optimized values of particles size distribution coefficients (q) and their corresponded values of visibility.

Table 1: Optimized Particles Size Distribution Coefficients (q) against Visibility

S/N	q	Visibility (km)
1	-0.87305488	0.1
2	-0.32520539	0.2
3	0.00473399	0.3
4	0.20107098	0.4
5	0.39901224	0.5

4.4 Improved Model

Equation (20) is the developed empirical model defines particle size coefficient distribution coefficient (q) at lower visibility. Consequently, (20) is the function defining visibility at $v < 0.5$ km. Therefore, (21) is the modified Kim's model of (11).

$$q = \begin{cases} 1.6 & \text{for } v > 50 \text{ km} \\ 1.3 & \text{for } 6 < v < 50 \text{ km} \\ 0.16v + 0.34 & \text{for } 1 < v < 6 \text{ km} \\ v - 0.5 & \text{for } 0.5 < v < 1 \text{ km} \\ 0.773429 \ln(v) + 0.9074367 & \text{for } v < 0.5 \text{ km} \end{cases} \quad (21)$$

4.5 Comparative Analysis

The performance of all the three (3) models in terms of attenuation against visibility was compared as shown in Figure 9. Equations (10) and (11) defined the values of (q) according to Kruse and Kim models respectively. Similarly, the new value of (q) at low visibility also defined by the improved model as given by (21). A common visibility point of 0.25 km was considered to determine the percentage improvement achieved on lowering the attenuation by the improved model in comparison with the existing mode ls as follows:

$$\text{Improve/Kruse Models} = \frac{32-20}{32} = 37.5\ \%$$

$$\text{Improve/Kim Models} = \frac{30-20}{30} = 33.33\ \%$$

Figure 10 shows that Kim's and Kruse's models presented similar characters with the developed improved model within the visibility range of $v \leq 0.5$ km. However, the developed improved model performed much better by achieving lower attenuation value than the existing models, whereby at visibility value of 0.01 km the corresponding a ttenuation value is approximately 100 dB/km with respect to Kruse and Kim models. The higher attenuation of nearly3000 dB/km.

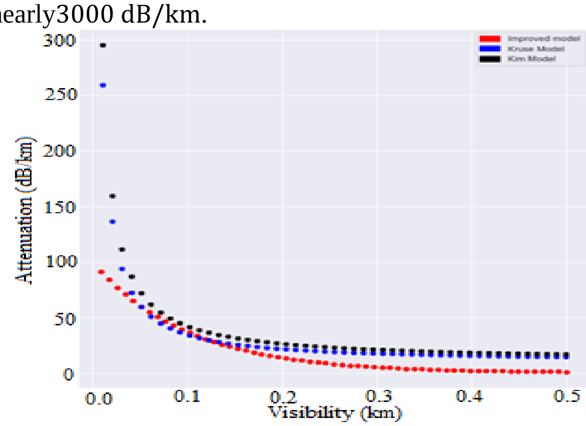

Figure 10: Attenuation at Low Visibility of the Developed in Comparison with the Other Models

Figure 11 illustrated how the developed model best fitted-in the trained measured data compared to the existing model as in Figure 11.

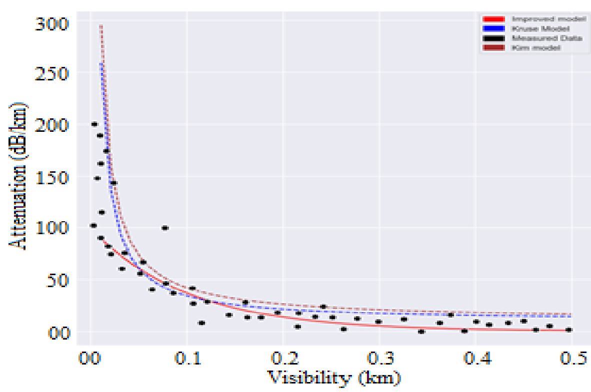

Figure 11: Measured of Fog Attenuation Coefficient as a Function of Visibility

5. Conclusion

This paper proposed to validate fog attenuation model in tropical. The new and improved models were developed, optimized and simulated with the sole aim of finding the optimum value(s) and the developed model validated. The results obtained were also compared with that of the existing models. It has been observed that the developed model achieved lowering the attenuations by 33,33% and 37.5% with respect to Kim and Kruse model respectively. The optimal values of q at visibility range of $0.3 < v < 0.5$ km are 0.00473399, 0.20107098 and 0.39901224. by maximizing the value of Particle size distribution coefficient. Lastly, the developed model is best fitted the measured data.

Further work is recommended especially in the area of lower visibility range of $0 < v < 0.2$ km. The research only achieved improvement within the visibility range of $0.2 < v < 0.5$ km.This will also further improve the overall system performance by reducing fog attenuation effect.

References

Adel M., Seleem H., Nasr M., and El Khobby., (2020), Transmission of 128 Gb/s Optical QPSK Signal over FSO Channel under Different Weather Conditions and Pointing Errors, Journal of Physics: Conference Series 1447 (2020) 012055, Tanta, Egypt. 1-7.

Chowdhury Z. M., Shahjalal Md., Hasan K. M., and Jang M.Y., (2019) The role of optical wireless communication technology in 5G/6G and IoT solution: prospects, direction, and challenges Journal of applied science. (Appl. Sci. 2019, 9, 4367). pp. 1-20.

Cisco (2020), Cisco Annual Internet Report, 2018 2023,whitepaper,onbroadband, Wi Fi, and mobile (3G, 4G, 5G) networking, pp.5 https://www.cisco.com/c/en/us/solutions/collateral/executiveperspectives/annual_internet report .

Gambo D., Tekanyi A.M.S., Musa M.J., Al- Mustapha M.D. and Ya'u I (2023) Beam Divergence Loss Mitigation in Free Space Optical Communication Channel Using Field of View Technique. Sule Lamido University Journal of Science & Technology Vol. 6 No. 1&2 [March, 2023], 30 43. https://doi.org/10.56471/slujst.v6i.344. Online ISSN: 2736-0903, Print ISSN: 2736 089X, www.slujst.edu.ng

Esmail A. M., Fathallah H. and Alouini M., (2016), Analysis of Fog Effects on Terre strial Free Space Optical Communicatio n Links, In: IEEE ICC 2016 Workshops: W02 Second Workshop on Optical Wireless Communications. King Abdulaziz City for Science and Technology (KACST), 34-45.

Fang J., Shilin M.B., Yang X.G., Liu L., Zhang Y., & Hu. W., (2018), Polar code MIMO FSO communication over gamma-gamma turbulence channel with spatial correlated fading. Journal of optical communication networks volume 10. No. 11. Optical society of America. pp. 915-923.

Farouk K., Shaker, and Ali M. A. A., (2019), Performance of Free Space Optical Communication Link under Foggy Weather, In: Journal of Communications, 14(6), Research Gate, 518-523.

Flecker B., Gebhart M., Leitgeb E., Muham mad S.S., and Chlestil C. (2015), Result s of attenuation measurements for Optical Wireless channels under dense fog conditions. regarding different wavelengths, Proc. of SPIE Vol. 6303 pp1-11.

Garcia S. I., (2018) An introduction to Descent Algorithm, Computer science engineer and Machine Learning enthusiast Retrieved from https://medium.com/@montjoile on 20/10/20, at 2:. 30pm.

Henniger H. & Wilfert O. (2010), An introduction to free space optical communication, journal of radio engineering, vol, 19, number 2, 203 – 212.

Ijaz M., Ghassemlooy Z., Perez J., Brazda V., and Fiser O. (2013a), Enhancing the Atmospheric Visibility and Fog Attenuation Using a Controlled FSO Channel, IEEE, Photonics Technology Letters, Vol. 25, No. 13, 2013.Pp 1262 – 1265.

Ijaz M., Ghassemlooy Z., Rajbhandari S., Le Minh H., Perez J., and Gholami A., (2012), Comparison of 830 nm and 1550nm based Free Space Optical link under Controlled Fog Conditions, 8th IEEE, Internation al Symposium on Systems, Networks and Digital Signal Processing, pp 4577-1473.

Ijaz M., Ghassemlooy1 Z.., Le-minh H., Zvanovec S., Perez J., Pesek J., and Fiser O., (2013b), Experimental Validation of Fog Models for FSO under Laboratory Controlled Conditions, 2013 IEEE 24th International Symposium on Personal, Indoor and Mobile Radio Communications: Fundamentals and PHY Track, pp.19-23.

Jahid A., Alsherif M. H., and Hall T.J., (2022), A contemporary survey on free space optical communication: Potential ,technical challenges, recent advances and research direction,Journal of networ k and computer applications, Science Direct, Elsevier, doi.org/10.1016/j.jnca. 2021.103311. 200 (22), 15-22.

Kashani M.A., Uysal M., and Kavehrad M., (2015), A novel statistical channel model for turbulence-induced fading in free-space optical systems, In: Journal of Light wave Technology. IEEE, 1-10.

Kaushal H., Jain, V. K., & Kar, S., (2017). Free Space Optical Communication, Opt ical Networks, Springer (India) Pvt. Ltd. DOI 10.1007/978-81-322-3691-7. Pp. 41-49.

Kaushal H. and Kaddoum G. (2016), Optical Communication in Space: Challenges and Mitigation Techniques. In Communications Surveys & Tutorials. pp. 1-41. IEEE.

Kedar D. and Arnon S. (2004). Urban optical wireless communication networks: the main challenges and possible solution. In Journal of Optical communication, pp. 52-57. IEEE.

Khalid H. S., Neil J.M., Peter S.E., Raed A.A., and Chan H. S., (2019) Antenna for emerging 5G system. In International journal of antenna and propagation pp 1-3.

Killinger D., (2002). Free space optics for laser communication through the air. In Optics & Photonics News, vol. 13, pp. 36-42.

Mingjian, C., Y., G., Jiangting, L., Xiaotong, Z., And Lixin G., (2018), Inverse Gaussian gamma distribution model for turbulence induced fading in free space optical communication. In Applied Optics, Vol. 57, No. 12 / 20, Optical Society of America, pp3031-3037.

Nigerian Communication Commission (NCC) (2020). An exploratory study on the challenges and survivability of ISP licensees in the Nigerian telecom se ctor, pp.5 5. Availableat https://www.ncc.gov.ng/accessible/documents/978 study on the challengesandsurvivability ofisplicensees-in-the-nigerian-telecom- sector/file Retrieved on 21-05-21.

Patnaik S., Srujanika S. S., Anshuman P., Chandni J., (2016), Free Space Optical Communication, A Review. In International Research Journal of Engineering and Technology (IRJET), Volume: 03, Issue: 04. pp 1261-1265.

Qadir Z., Saeed N., Munawar H.S. (2021), Towards 6G Internet of Things: Recent Advances, Use Cases, and Open Challenges. www.sciencedirect.com, 2022. Pp. 1-16.

Rockwell D. A., & Mecherle G. S., (2001), Optical wireless: low cost high speed op tical access Asia pacificoptical and wire less communications conference and exhibit, volume 4586, pp.11 15. Retrieved fromhttps://www.spiedigitallibrary.or g/conference-proceedings-of-spie.

Shaker F. K., and Ali M. A. A. (2019), Performance of Free Space Optical Communication Link under Foggy Weather, Journal of Communications Vol. 14, No. 6, June 2019, pp.518-523-135.